

Modeling & Simulation of Fuel-Cell Stacked Cascaded H-Bridge High Level Inverter for Electric Vehicle

Om Shiv Verma

M.Tech Scholar (Control System)
NITM, (RGPV) Gwalior, (M.P.)
Email: omshivbiet@gmail.com

Rameshwar Singh

Assist. Professor, Dept. of Electrical Engineering
NITM, (RGPV) Gwalior, (M.P.)
Email: rameshwar.gwalior@gmail.com

Abstract – Proton exchange membrane (PEM) fuel cell is one of the promising and technologies in coming future for alternative source of power generation. As fuel cells are a source of DC voltage but for many applications AC supply is required and hence inverter circuit fed by a fuel cell is important. Multilevel inverter is a promising topology to generate waveforms close to a sinusoid. Among the multilevel inverter topologies, cascaded multilevel inverter requires the least number of switches and dc sources. The main focus of this paper is to develop an electrical model of the fuel cell supplying a cascade multilevel inverter. The fuel cell stack and reformer model is simulated using MATLAB and the eleven-level inverter output is verified using fuel cell as the power source. Furthermore, to control the power flow of fuel cell system a PID controller is used. Among various modulation strategies, and this paper focuses on the PWM method because it is less complex hence reliable and easy to implement. Simulation results confirmed the high performance of the controller to control power generation. Both the inverter circuit topology and its control scheme are described in detail and their performance is verified based on simulation and results.

Keywords – MATLAB, PEMFC, PID Controller, PWM, Fuel Cell.

I. INTRODUCTION

Electricity plays an important role in modern society since it was first used about one century ago. To utilize electricity for all kinds of tasks, many different electrical and electronic devices have been invented. Among these, the DC-AC converter is one of the most important power electronic devices.

Automobiles are the integral part of daily life as it provides freedom of mobility. Automotive industries' solution to this problem is the electric vehicles (EVs), which are zero emission vehicles, and the hybrid electric vehicles (HEVs), which emit low amounts of environmentally harmful gases such as CO, CO₂ and NO_x. Electric vehicles require batteries as the energy source. Batteries need to be recharged after electric vehicles operate for a few hours. [1] Pure electric cars have demerits such as a short driving distance, long recharging time, and high cost. Thus, fuel cell vehicles (FCV), which have a longer distance and higher transportation capability than pure electric cars. FCV is one type of electric vehicles with fuel cell system which is the main generating unit. A hydrogen-based, fuel cell provides the power to give an electric vehicle the same range as a gasoline powered vehicle. In this case, a fuel cell stack generates the electricity by combination of

hydrogen and oxygen. [2] The products of the electrochemical process are electricity, heat and water. Polymer Electrolyte Membrane Fuel Cell (PEM Fuel Cell) is popular and suitable used in vehicles. It operates within a range of relatively low temperatures, has higher efficiency than combustion engines, is very quiet and produces no emissions. [3]

1.1 Fuel Cell:

A fuel cell is an electrochemical energy conversion device. A fuel cell converts the chemicals hydrogen and oxygen into water, and in the process it produces electricity. Most fuel cells in use today use hydrogen and oxygen as the chemicals. The proton exchange membrane fuel cell (PEMFC) is one of the most promising technologies. This is the type of fuel cell that will end up powering cars, buses and maybe even your house. The PEMFC uses one of the simplest reactions of any fuel cell.

- The anode, the negative post of the fuel cell, has several jobs. It conducts the electrons that are freed from the hydrogen molecules so that they can be used in an external circuit.
- The cathode, the positive post of the fuel cell, has channels etched into it that distribute the oxygen to the surface of the catalyst and form water. The catalyst is a special material that facilitates the reaction of oxygen and hydrogen. It is usually made of platinum powder very thinly coated onto carbon paper or cloth
- The electrolyte is the proton exchange membrane. This specially treated material, which looks something like ordinary kitchen plastic wrap, only conducts positively charged ions. The membrane blocks electrons.

The open circuit voltage calculation is based on the Nernst equation having the following form:

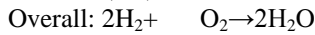
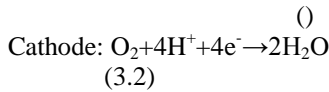
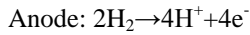
$$V_{oc} = V_{oc}^o + \frac{RT}{2F} \ln \left(\frac{\frac{P_{H_2}}{P^o} \left(\frac{P_{O_2}}{P^o} \right)^{\frac{1}{2}}}{\frac{P_{H_2O}}{P_{H_2O}^o}}} \right) \quad (1)$$

where V_{oc}^o is the open circuit voltage at standard pressure P^o and temperature T , R is the molar gas constant, F is the Faraday constant, P_{H_2} , P_{O_2} and P_{H_2O} are partial pressures of hydrogen, oxygen and water vapour respectively and $P_{H_2O}^o$ is the saturation pressure of water at the temperature T . The open circuit voltage at standard pressure is calculated according to:

$$V_{oc}^o = \frac{-g_f}{2F} \quad (2)$$

where g_f is the Gibbs free energy of formation for the fuel cell reaction

The chemical reactions in the PEM fuel cell can be described as:



The operational voltage V_{fc} is calculated by subtracting from the open circuit voltage of equation (22) the losses associated with operational conditions. These losses are the ohmic losses ΔV_{ohm} due to electric and ohmic resistance, the activation losses ΔV_{act} associated with driving the chemical reaction and the mass transportation losses ΔV_{mass} caused by the changes in concentration of the reactants and products. The losses are calculated according to:

$$\Delta V_{ohm} = ir_f \quad (3)$$

$$\Delta V_{act} = A_f \ln\left(\frac{i}{i_0}\right) \quad (4)$$

$$\Delta V_{mass} = me^{ni} \quad (5)$$

where i is the current density. The values of the constants used in the calculations are summarized in table 7 [14]. Using the equations above the operational voltage can be calculated according to:

$$V_{fc} = V_{oc} - \Delta V_{ohm} - \Delta V_{act} - \Delta V_{mass} \quad (6)$$

$$V_{fc} = V_{oc} - ir_f - A_f \ln\left(\frac{i}{i_0}\right) - me^{ni} \quad (7)$$

$$V_{fc} = \frac{-g_f}{2F} + \frac{RT}{2F} \ln\left(\frac{\frac{P_{H_2}}{P^o} \left(\frac{P_{O_2}}{P^o}\right)^{\frac{1}{2}}}{\frac{P_{H_2O}}{P^o}}}\right) + A_f \ln(i_0) - ir_f - A_f \ln(i) - me^{ni} \quad (8)$$

Using the form of equation (29) it is possible to adapt the operational voltage calculation to the results of experimental measurements on a specific fuel cell. In this study literature data are used, since such experiments are not performed. Figure 9 shows the cell voltage as a function of current for the fuel cell used in the model.

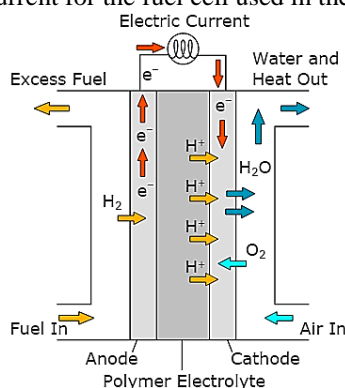


Fig.1. Fuel Cell Model

This reaction in a single fuel cell produces only about 0.7 volts. To get this voltage up to a reasonable level, many separate fuel cells must be combined to form a fuel-cell stack.

1.2 Fuel Cell Stack:

The cells' peak power is 14.25 kW per sub-stack, and 85.5kW total .Fuel cell efficiencies vary between 50 percent at 0.6V/cell and 67 percent at 0.8V/cell. Specific energy is dependent on the quantity of hydrogen available to feed the fuel cell. Current density is 0.94A/cm at 0.6V/cell.

II. FUEL CELL STACK PARAMETERS DETERMINATION

For the simplified model, four parameters (E_{oc} , V_1 , i_0 , NA) are to be determined which requires at least four simultaneous equations. The following sets of equations are:

$$V_1 = E_{oc} + NA \ln i_0 - R_{ohm} I_{nom} \quad (9)$$

$$V_{nom} = E_{oc} - NA \ln\left(\frac{I_{nom}}{i_0}\right) - R_{ohm} I_{nom} \quad (10)$$

$$NA = \frac{(V_1 - V_{nom})(I_{max} - 1) - (V_1 - V_{min})(I_{nom} - 1)}{\ln(I_{nom})(I_{max} - 1) - \ln(I_{max})(I_{nom} - 1)} \quad (11)$$

$$R_{ohm} = \frac{V_1 - V_{nom} - NA \ln(I_{nom})}{I_{nom} - 1} \quad (12)$$

$$i_0 = e^{\left(\frac{V_1 - E_{oc} + R_{ohm}}{NA}\right)} \quad (13)$$

$$\eta = \frac{nFV_{nom}}{\Delta h^\circ(H_2O(gas))N} \times 100 \quad (14)$$

2.1 DC-DC Converter:

The DC/DC converter is voltage-regulated. The DC/DC converter adapts the low voltage of the battery (200 V) to the DC bus which feeds the AC motor. A DC-DC converter is a device that accepts a DC input and produces a DC output voltage. It would be step-down (Bust) converter to lower input voltage, or step-up (Boost) converter to increase input voltage.

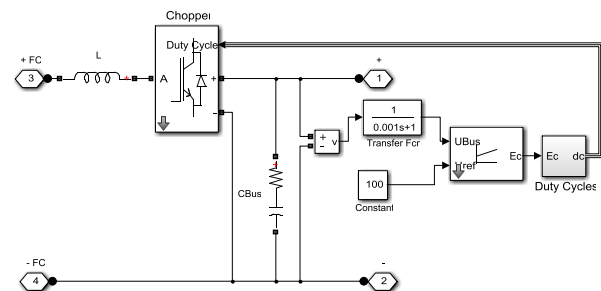


Fig.2. DC-DC Boost Converter

2.2 Multilevel Inverter:

In recent years, multilevel converters have been developed for several reasons.

The multilevel converter is one of the more promising techniques for mitigating the aforementioned problems. Multilevel converters utilize several DC voltages to synthesize a desired AC voltage.

One application for multilevel converters is distributed power systems. Multilevel converters can be implemented using distributed energy resources such as photovoltaic and fuel cells, and then be connected to an AC power grid. If a multilevel converter is made to either draw or supply purely reactive power, then the multilevel converter can be used as a reactive power compensator. For example, a multilevel converter being used as a reactive power compensator could be placed in parallel with a load connected to an AC system. This is because a reactive power compensator can help to improve the power factor of a load [14].

2.3 H-Bridge Inverter:

The control of cascaded H-bridge structure is simple, and this structure does not have DC voltage-equalizing problems. So the cascaded H-bridge structure is widely used in large-capacity high-voltage power electronic devices.

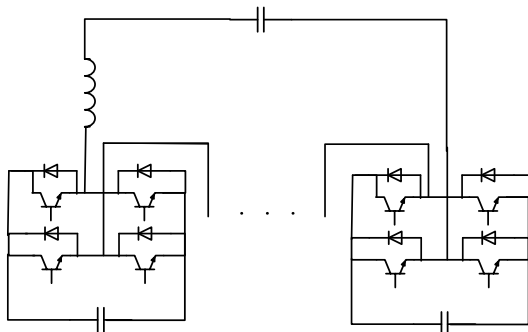


Fig.3. Diagram of cascaded H-bridge

III. TOPOLOGY OF MULTILEVEL CONVERTERS

3.1 Diode-Clamped Converter

The simplest diode-clamped converter is commonly known as the neutral point clamped converter (NPC) which was introduced by Nabae *et al.* [4]. The NPC consists of two pairs of series switches (upper and lower) in parallel with two series capacitors where the anode of the upper diode is connected to the midpoint (neutral) of the capacitors and its cathode to the midpoint of the upper pair of switches; the cathode of the lower diode is connected to the midpoint of the capacitors and divides the main DC voltage into smaller voltages, which is shown in Figure 4. In this example, the main DC voltage is divided into two. If the point *O* is taken as the ground reference, the three possible phase voltage outputs are $-1/2V_{dc}$, 0, or $1/2V_{dc}$. The line-line voltages of two legs with the capacitors are: V_{dc} , $1/2V_{dc}$, 0, $-1/2V_{dc}$ or

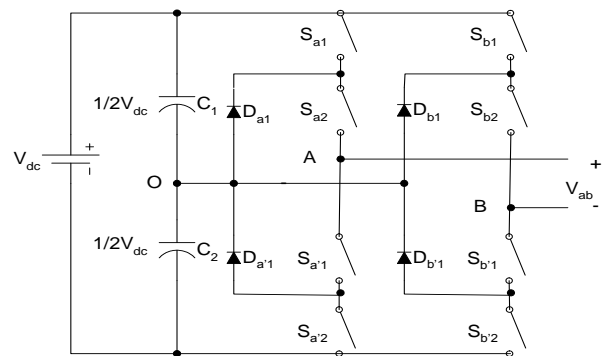


Fig.4. Neutral point diode-clamped converter

3.2 Capacitor-Clamped Converter

The capacitor-clamped multilevel converter or flying-capacitor converter [6], [12] is similar to the diode-clamped topology, which is shown in Figure 2.3. However, the capacitor-clamped multilevel topology allows more flexibility in waveform synthesis and balancing voltage across the clamped capacitors. For a three-level capacitor-clamped multilevel converter, if the *O* point is taken as the ground reference, a single phase can produce three output levels ($-1/2V_{dc}$, 0 and $1/2V_{dc}$). The general *m*-level capacitor-clamped multilevel converter has an *m*-level output phase voltage. Thus, two phases would produce a $(2m - 1)$ level output voltage, or line voltage, which is shown in Figure 2.4. Similar to the diode-clamped multilevel converter, the capacitors have different ratings. These capacitors result in a bulky, and expensive converter when compared to the diode-clamped converter.

The configuration has mixed-level hybrid multilevel units because it embeds multilevel cells as the building block of the cascade converter.

Although it is possible to reduce the harmonic contents with less cascaded cells required for unequal DC sources multilevel converters, the control for unequal DC sources multilevel converters is very complicated. Until now, most of the available control methods are for equal DC sources multilevel converters. This is its main disadvantage.

IV. CLASSIFICATION OF MODULATION STRATEGIES MULTILEVEL CONVERTERS

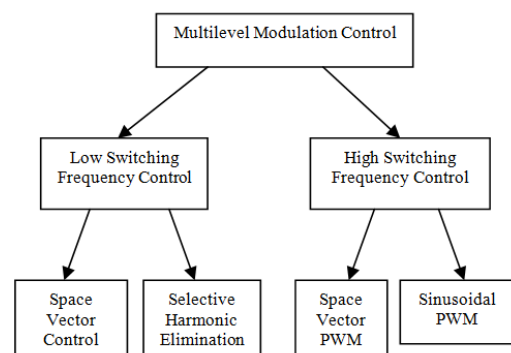


Fig.5. Classification of multilevel modulation methods

One of the most widely used strategies for controlling the AC output of power electronic converters is the technique known as pulse width modulation (PWM), which varies the duty cycle of the converter switches at a high switching frequency to achieve a target average low-frequency output voltage or current. Three significantly different PWM methods for determining the converter switching ON times have been usefully proposed for fixed-frequency modulation systems [1]

4.1 Selective Harmonic Elimination

The popular selective harmonic elimination method is also called fundamental switching frequency method which is based on the harmonic elimination theory developed by Patel *et al* [28][29].

By applying Fourier series analysis, the output voltage can be expressed as

$$V(t) = \sum_{n=1,3,5,\dots}^{\infty} \frac{4}{n\pi} (V_1 \cos(n\theta_1) + V_2 \cos(n\theta_2) + \dots + V_s \cos(n\theta_s)) \sin(n\omega t) \quad (15)$$

where s is the number of DC sources, and V_1, V_2, \dots, V_s are the level of DC voltages. The switching angles must satisfy the condition $0 < \theta_1 < \theta_2 < \dots < \theta_s < \frac{\pi}{2}$. However,

if the switching angles do not satisfy the condition, this method no longer exists. If $V_1 = V_2 = \dots = V_s$, this is called equal DC voltages case. To minimize harmonic distortion and to achieve adjustable amplitude of the fundamental component, up to $s-1$ harmonic contents can be removed from the voltage waveform. In general, the most significant low-frequency harmonics are chosen for elimination by properly selecting angles among different level converters, and high-frequency harmonic components can be readily removed by using additional filter circuits. To keep the number of eliminated harmonics at a constant level, all switching angles must satisfy the condition $0 < \theta_1 < \theta_2 < \dots < \theta_s < \frac{\pi}{2}$, or the total harmonic

distortion (THD) increases dramatically. Due to this reason, this modulation strategy basically provides a narrow range of modulation index, which is one of its disadvantages [13].

By applying Fourier series analysis, the output voltage can be expressed as

$$V(t) = \sum_{n=1,3,5,\dots}^{\infty} \frac{4}{n\pi} (V_1 \cos(n\theta_1) \pm V_2 \cos(n\theta_2) \pm V_3 \cos(n\theta_3) \pm \dots \pm V_s \cos(n\theta_s)) \sin(n\omega t) \quad (16)$$

where s is the number of switching angles, and V_1, V_2, \dots, V_s are the level of DC voltages. In this expression, the positive sign implies the rising edge, and the negative sign implies the falling edge. Similar to the fundamental switching frequency method, the switching angles must satisfy the condition $0 < \theta_1 < \theta_2 < \dots < \theta_s < \frac{\pi}{2}$. However, if

the switching angles do not satisfy the condition, this method no longer exists.

Therefore, the modulation control problem is converted into a mathematic problem to solve the following

equations for a three-phase system. Here, m is modulation index.

$$V_1 \cos(\theta_1) \pm V_2 \cos(\theta_2) \pm V_3 \cos(\theta_3) \pm \dots \pm V_s \cos(\theta_s) = m$$

$$V_1 \cos(5\theta_1) \pm V_2 \cos(5\theta_2) \pm V_3 \cos(5\theta_3) \pm \dots \pm V_s \cos(5\theta_s) = 0$$

⋮

$$V_1 \cos(n\theta_1) \pm V_2 \cos(n\theta_2) \pm V_3 \cos(n\theta_3) \pm \dots \pm V_s \cos(n\theta_s) = 0 \quad (17)$$

4.2 Model Description:

Here in the model the fuel cell stacks are cascaded to maintain the voltage level up to the requirement. There are three segments arranged so that the three phase power can be generated. First of all the fuel cell generated dc voltages is step-up by using dc-dc boost converter and then it is converted to ac voltage by using H-Bridge inverter. Basically model has divided into three major parts named as: Fuel cell, dc-dc boost converter and H-Bridge inverter.

In the proposed work five fuel cell stacks are cascaded for single phase so that the gain is to be made up to the required limit, in the same way for all the remaining phases it is done.

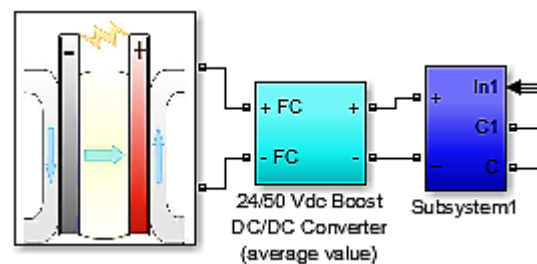


Fig.6. Proposed Model Block Diagram

The dc-dc boost converter is designed in such a way that the voltage level can be lifted up to the required limit by optimal switching, generated by the PWM generation subsystem. Now this lifted dc voltage is inverted into ac with eleven levels by inverter. Another important part or subsystem of the complete system is present to generate switching pulse train for dc-dc boost converter and inverter.

V. SIMULATION RESULTS

The high multilevel output approaches the sinusoidal signal and the THD value reduces. Here the response of the

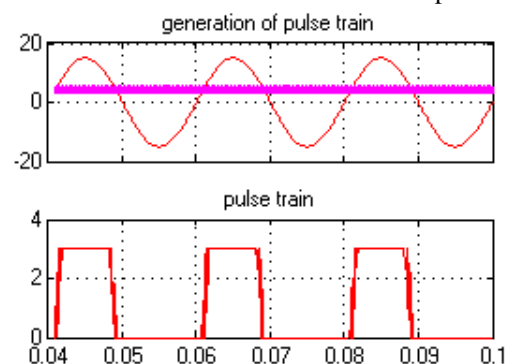


Fig.7. Generation of Pulse Train

first part is shown, which is actually designed to generate the pulse train for switching the inverter IGBTs. Each and every pulse is of about .08 sec.

The pulse train is for all the five inverters used in the phase A, B or C identically is shown in the figure (8). Pulse train is generated with the help of PWM generator. Every pulse is dedicated to the corresponding converter existing in the cascaded form.

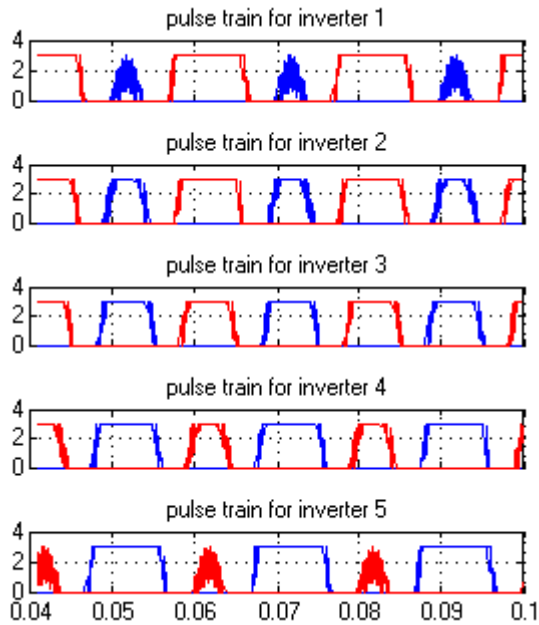


Fig.8. Pulse Train to the Inverter

In figure (9, 10 & 11) the phase A, phase B & phase C output is shown, the output dependent on the dc voltage. Here ac voltage is not proper; the peak output voltage is 230 volt.

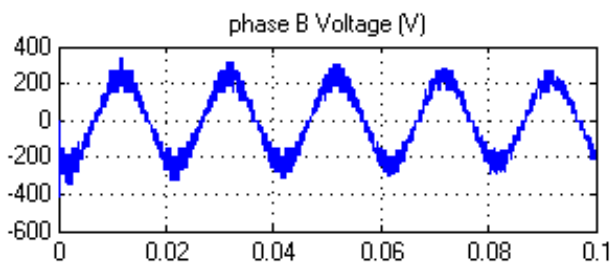


Fig.9. First Phase waveform without improvement)
Distortion is present in the output voltage waveforms.

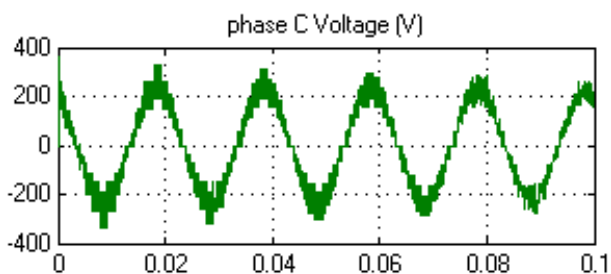


Fig.10. Second Phase waveform without improvement

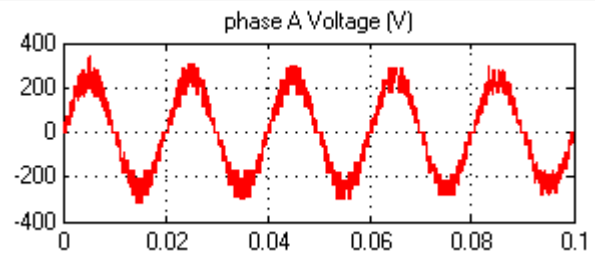


Fig.11. First Phase waveform without improvement

In figure (12) combined three phase output voltage waveforms is shown, this is the output which is the individual response of all the three subparts of the system. The three phase output is in proper in phase which is done with the proper switching, only the distortion is present with in it.

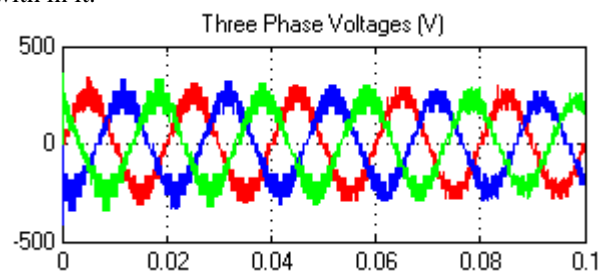


Fig.12. Combined Phase waveform without improvement

As per the waveform conditioning sub-system the distorted output is improved, in fig (13) blue colour waveform shows the unconditioned output voltage while as red colour waveform shows the conditioned output voltage.

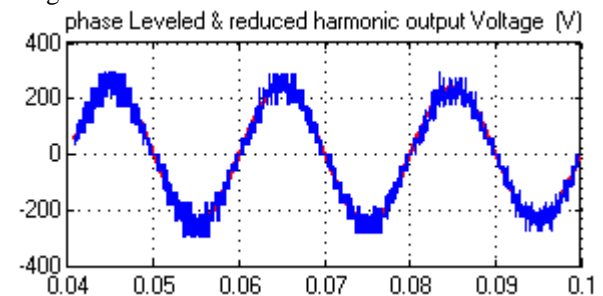


Fig. 13. Actual and improved output voltage waveforms

In figure (14) the improved output voltage is shown below, here we can see that the output voltage is more proper and the quality of the output is measures in the form of THD value. So it is most accurate high level output voltage.

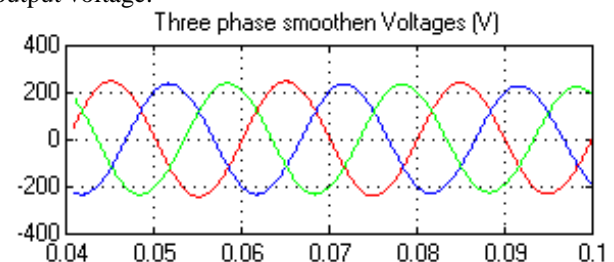


Fig.14. Combined improved output voltage waveforms

The FFT analysis is done to calculate the THD value to know about the quality of the output voltage, here firstly the FFT analysis of the actual non-improved signal is performed and THD is found 15.91% of the fundamental. Here the higher order harmonics are reduced but in limited extent.

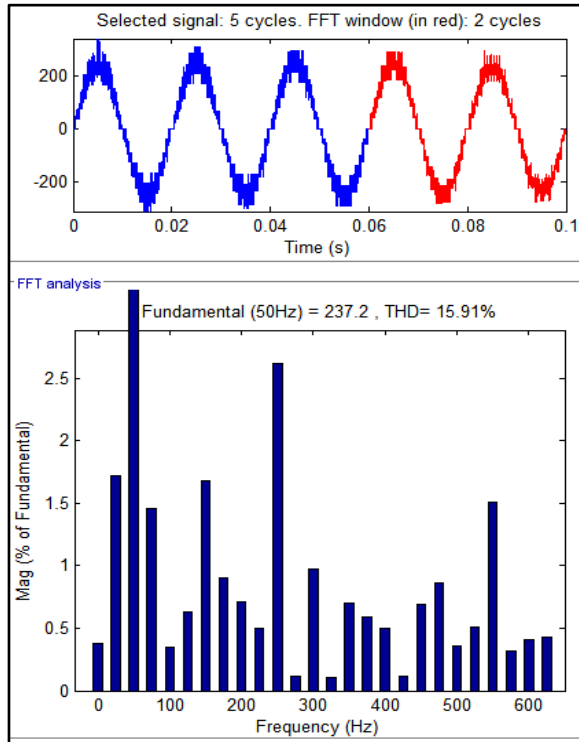


Fig.15. FFT analysis of actual output voltage waveforms

Here it is clear that the second harmonic is of .35% of the fundamental, third harmonic is of 1.68% of the fundamental, fourth harmonic is of .72% of the fundamental, fifth harmonic is of 2.62% of the fundamental and seventh harmonic is of .70% of the of the fundamental.

From the figure (15) & figure (16) it is analyzed and clear that the odd level harmonics are dominating and these harmonics degrading the power quality.

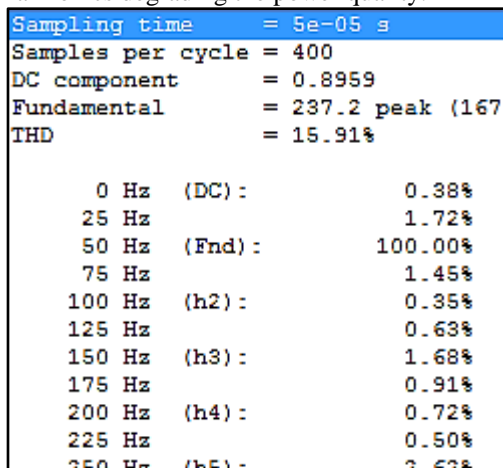


Fig.16. FFT analysis of actual output voltage waveforms

In case, as the improvement is done the output voltage is improved and THD is found .95% of the fundamental. The THD value is minimized up to a great extent with the reduction of higher order harmonics as shown in FFT window in figure (17).

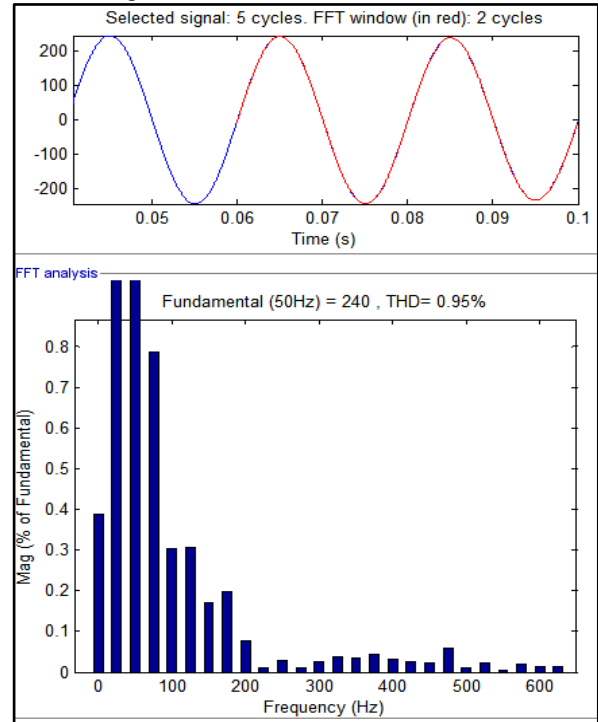


Fig.17. FFT analysis of Improved output voltage waveforms

The FFT window shown in figure (18), we can see that the even and odd level harmonics are minimized as compare to the above.

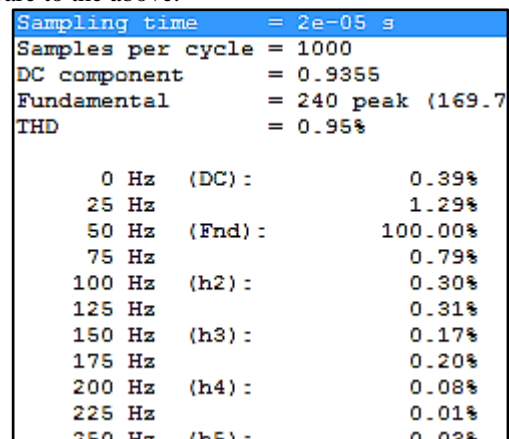


Fig.18. FFT analysis of Improved output voltage waveforms

VI. CONCLUSION

The current trend of modulation control for multilevel converters is to output high quality power with high efficiency. For this reason, popular traditional PWM, sinusoidal PWM (SPWM) methods and space vector PWM (SVPWM) methods are not the best methods for

multilevel converter control due to their high switching frequency. The resultant method can solve low order harmonic equations, but cannot solve high order harmonic equations. In this thesis, switching angles for each H-Bridge converter are equal. If the switching angle numbers for each H-Bridge converter are not equal, it may be possible to find more solutions for a wider modulation index range. Here in the proposed work the signal improvement is done to make output signal proper. The THD is reduced up to significant extent i.e. from 15.91% to .95% without using any physical filter.

FUTURE WORK

This work focuses on harmonic elimination for multilevel converters with a preset switching scheme. Here the 11 level fuel cell based multilevel inverter is designed and we analyzed the performance regarding power quality issues. This work can be best utilized in the electric vehicles and other domestic applications where

REFERENCES

- [1] PeigenTian, Xi Xiao, Kui Wang, and Ruoxing Ding “A Hierarchical Energy Management System Based on Hierarchical Optimization for Microgrid Community Economic Operation” IEEE TRANSACTIONS ON SMART GRID Digital Object Identifier 10.1109/TSG.2015.2470551.
- [2] I.J.M. Besselink, P.F. van Oorschot, E. Meinders, and H. Nijmeijer, Design of an efficient, low weight battery electric vehicle based on a VW Lupo 3L, Battery, Hybrid and Fuel Cell Electric Vehicle Symposium & Exhibition, Shenzhen, China : 2010.
- [3] D. G. Holmes and T. A. Lipo, *Pulse width modulation for power converters*, IEEE press, 2003.
- [4] L. M. Tolbert, F. Z. Peng, T. G. Habetler, “Multilevel Converters for Large Electric Drives,” *IEEE Transactions on Industry Applications*, vol. 35, no. 1, Jan./Feb. 1999, pp. 36-44.
- [5] P. N. Enjeti, P. D. Ziogas, J. F. Lindsay, “Programmed PWM Techniques to eliminate Harmonics: A Critical Evaluation,” *IEEE Transactions on Industry Applications*, vol. 26, no. 2, March/April. 1990. pp. 302 – 316.
- [6] A. Nabae, I. Takahashi, and H. Akagi, “A new neutral-point clamped PWM converter,” *IEEE Transactions on Industry Applications*, vol. IA-17, pp. 518–523, Sept./Oct. 1981.
- [7] X. Yuan, H. Stemmler, and I. Barbi, “Investigation on the clamping voltage self-balancing of the three-level capacitor clamping converter,” in Proc. *IEEE PESC’99*, 1999, pp. 1059–1064.
- [8] C. Hochgraf, R. Lasseter, D. Divan, and T. A. Lipo, “Comparison of multilevel converters for static var compensation,” in Conf. Rec. *IEEE-IASAnnu.Meeting*, Oct. 1994, pp. 921–928.
- [9] P. Hammond, “A new approach to enhance power quality for medium voltage ac drives,” *IEEE Transactions on Industry Applications*, vol. 33, pp. 202–208, Jan./Feb. 1997.
- [10] E. Cengelci, S. U. Sulistijo, B. O. Woom, P. Enjeti, R. Teodorescu, and F. Blaabjerger, “A new medium voltage PWM converter topology for adjustable speed drives,” in Conf. Rec. *IEEE-IASAnnu. Meeting*, St. Louis, MO, Oct. 1998, pp. 1416–1423.
- [11] F. Z. Peng, “A generalized multilevel converter topology with self-voltage balancing,” *IEEE Transactions on Industry Applications*, vol. 37, pp. 611–618, Mar./Apr. 2001.
- [12] W. A. Hill and C. D. Harbourt, “Performance of medium voltage multilevel converters,” in Conf. Rec. *IEEE-IASAnnu. Meeting*, Phoenix, AZ, Oct. 1999, pp. 1186–1192.
- [13] M. D. Manjrekar, P. K. Steimer, and T. A. Lipo, “Hybrid multilevel power conversion system: a competitive solution for high-power applications,” *IEEE Transactions on Industry Applications*, vol. 36, pp. 834–841, May/June 2000.
- [14] J. S. Lai and F. Z. Peng, “Multilevel converters – A new breed of power converters,” *IEEE Transactions on Industry Applications*, vol. 32, no. 3, May/June 1996, pp. 509-517.
- [15] J. Rodríguez, J. Lai, and F. Peng, “Multilevel converters: a survey of topologies, controls and applications,” *IEEE Transaction on Industrial Electronics*, vol. 49, no. 4, Aug. 2002, pp. 724-738.
- [16] K. J. McKenzie, “Eliminating harmonics in a cascaded H-bridges multilevel converter using resultant theory, symmetric polynomials, and power sums,” Master thesis, 2004.
- [17] Feel-soon Kang, Sung-Jun Park, Kim, C.-U., “Multilevel converter employing cascaded transformers”, in *IEEE IECON*. Roanoke, Virginia, Nov. 2003, pp. 2185 – 2190.
- [18] B. Ozpineci, Z. Du, L. M. Tolbert, D. J. Adams, and D. Collins, “Integrating Multiple Solid Oxide Fuel Cell Modules”, *IEEE IECON*.Roanoke, Virginia, Nov. 2003, CD-ROM.
- [19] L. M. Tolbert, J. N. Chiasson, K. McKenzie, Z. Du, “Elimination of Harmonics in a Multilevel Converter with Non Equal DC Sources,” *IEEE Applied Power Electronics Conference (APEC 2003)*, February 9-13, 2003, Miami, Florida, pp. 589-595.
- [20] C. K. Duffey, R. P. Stratford, “Update of harmonic standard IEEE-519: IEEE recommended practices and requirements for harmonic control in electric power systems,” *IEEE Transactions on Industry Applications*, vol. 25, no. 6, Nov./Dec. 1989, pp. 1025-1034.
- [21] J. N. Chiasson, L. M. Tolbert, K. J. McKenzie, Z. Du, “A Complete Solution to the Harmonic Elimination Problem,” *IEEE Transactions on Power Electronics*, March 2004, vol. 19, no. 2, pp. 491-499.
- [22] J. N. Chiasson, L. M. Tolbert, K. J. McKenzie, Z. Du, “Control of a Multilevel Converter Using Resultant Theory,” *IEEE Transactions on Control System Theory*, vol. 11, no. 3, May 2003, pp. 345-354.
- [23] J. N. Chiasson, L. M. Tolbert, K. J. McKenzie, Z. Du, “A New Approach to Solving the Harmonic Elimination Equations for a Multilevel Converter,” *IEEE Industry Applications Society Annual Meeting*, October 12-16, 2003, Salt Lake City, Utah, pp. 640-645.